Anderson localization of ballooning modes, quantum chaos and the stability of compact quasiaxially symmetric stellarators

M. H. Redi, J. L. Johnson, S. Klasky, J. Canik, R. L. Dewar, and W. A. Cooper

Citation: Physics of Plasmas (1994-present) **9**, 1990 (2002); doi: 10.1063/1.1448344
View online: http://dx.doi.org/10.1063/1.1448344
View Table of Contents: http://scitation.aip.org/content/aip/journal/pop/9/5?ver=pdfcov
Published by the AIP Publishing

Anderson localization of ballooning modes, quantum chaos and the stability of compact quasiaxially symmetric stellarators[a)]

M. H. Redi,[b)] J. L. Johnson, and S. Klasky
Plasma Physics Laboratory, Princeton University, P.O. Box 451, Princeton, New Jersey 08543

J. Canik
Department of Electrical and Computer Engineering, University of Wisconsin, Madison, Wisconsin 53706

R. L. Dewar
Department of Theoretical Physics, The Australian National University, Canberra, ACT 0200, Australia

W. A. Cooper
Ecole Polytechnique Federale de Lausanne, CH-1007, Lausanne, Switzerland

(Received 25 October 2001; accepted 3 December 2001)

The radially local magnetohydrodynamic (MHD) ballooning stability of a compact, quasiaxially symmetric stellarator (QAS), is examined just above the ballooning beta limit with a method that can lead to estimates of global stability. Here MHD stability is analyzed through the calculation and examination of the ballooning mode eigenvalue isosurfaces in the 3-space (s,α,θ_k); s is the edge normalized toroidal flux, α is the field line variable, and θ_k is the perpendicular wave vector or ballooning parameter. Broken symmetry, i.e., deviations from axisymmetry, in the stellarator magnetic field geometry causes localization of the ballooning mode eigenfunction, and gives rise to new types of nonsymmetric eigenvalue isosurfaces in both the stable and unstable spectrum. For eigenvalues far above the marginal point, isosurfaces are topologically spherical, indicative of strong ''quantum chaos.'' The complexity of QAS marginal isosurfaces suggests that finite Larmor radius stabilization estimates will be difficult and that fully three-dimensional, high-n MHD computations are required to predict the beta limit. © *2002 American Institute of Physics.*
[DOI: 10.1063/1.1448344]

I. INTRODUCTION

The stability and confinement of plasma configurations are key issues for the success of the magnetic confinement fusion energy program. Classical stellarators were found to have unacceptably poor particle confinement many decades ago, but new concepts and methods for designing magnetic configurations, due to Nührenberg[1] and Garabedian,[2] have led to quasisymmetric stellarators with computationally drift-orbit-optimized confinement. Just as symmetry is known to govern particle transport and system stability throughout mathematical physics (e.g., Noether's theorem[3]) and all branches of contemporary physics, it is central to the development of these new stellarator designs. Plasma beta (β) is a measure of performance, defined as the confined plasma kinetic energy divided by the confining magnetic energy of a fusion device. The problems of disruptions and magnetohydrodynamic (MHD) stability which limit β for axisymmetric tokamak performance are also central to stellarator design and, like particle transport, can be targeted with computational optimization techniques. Here we explore some aspects of the effect of symmetry and optimized stellarator design on MHD ballooning mode stability properties for a proposed, next generation, medium size stellarator experiment.

The National Compact Stellarator Experiment (NCSX)[4] is a hybrid configuration which is intended to combine the best features of drift-orbit-optimized stellarators, and advanced tokamaks. For the new stellarators, global kink and vertical mode high-n MHD stability can be calculated in the ideal, linear limit[5,6] for fully three-dimensional configurations. Simpler, one-dimensional, radially local, ballooning calculations provide rapid estimates of MHD stability,[7] but are likely to underestimate the maximum average β achievable. The quasiaxially symmetric stellarator (QAS) design for NCSX has β limited by high-n kink and ballooning instabilities. Consequently, a detailed study of ballooning stability is of interest for this QAS design, with the aim of understanding and increasing the β limit.

In this paper we report on the application to the QAS of a well-known approach[8] to investigating ballooning mode spectra which has recently been applied to stellarators,[9,10] enhanced by new high performance computing and visualization tools. The method makes use of the additional geometric and profile information contained in the results of a large set of *local* ballooning eigenvalue calculations to infer *global* mode stability. Ballooning eigenvalue isosurfaces have been found which exhibit radial, poloidal, and toroidal localization[9] for the H-1NF heliac[11] at The Australian National University and for 10 field period stellarators[10,12] related to the large helical device (LHD)[13] in Japan. Given these isosurfaces, ray tracing can be used to predict the oc-

[a)]Paper QI1 5, Bull. Am. Phys. Soc. **46**, 247 (2001).
[b)]Invited speaker. Electronic mail: redi@pppl.gov

currence of kinetic stabilization of β for a plasma configuration.

The symmetry breaking localization of the unstable ballooning mode eigenfunction in stellarator plasmas has been shown to be analogous to the disorder-driven Anderson localization[14] of one dimensional quantum systems. This eigenfunction localization, driven by departure from periodicity in the equilibrium, is important in condensed matter physics, as well as in acoustics and nonlinear optics. Abstract mathematical concepts and terminology, not usually found in plasma physics (broken symmetry, localization of eigenfunctions, quantum chaos, eigenvalue isosurface topologies), have crossed the boundaries of scientific subfields and provide new methods with which to investigate stability in plasma physics.

The paper is organized as follows. In Sec. II we describe the QAS configuration and discuss MHD instability calculations of ballooning mode stability. Section III presents results for the localized eigenfunctions and structures found in the QAS energy spectra above the design point average β. These are compared to other stellarators and to axisymmetric tokamaks. In Sec. IV we discuss these results, the possibility of finite Larmor radius stabilization of the ballooning instability in the QAS and comment on the connections between symmetry breaking and the practical problems of plasma particle confinement and MHD stability.

II. QAS BALLOONING MODE STABILITY CALCULATIONS

The symmetric stellarator concept has led to improved toroidal plasma configurations, for which good particle confinement has been of primary importance. With sufficient field line rotational transform iota ($\iota = 1/q$), good neoclassical particle confinement is assured. Unfortunately, tokamaks require a large toroidal current to provide rotational transform, but such high current, necessary for high performance plasmas, leads to instabilities and disruptions. The new designs for the QAS stellarator are planned to provide rotational transform by modular field coils as well as bootstrap current, and so are both more stable to the kink mode and support steady state operation.

The National Compact Stellarator Experiment (NCSX) design point[4] is similar to the three-dimensional QAS plasma configuration we examine. The stellarator plasma configuration at 4% β is found to have good particle confinement as well as kink, vertical and ballooning stability. This drift–orbit optimized experiment would be complementary to the large experiments underway in Japan (LHD) and under construction in Germany [Wendelstein-7-X (W-7X)],[15] as well as to a smaller symmetric stellarator in Wisconsin [the Helically Symmetric Stellarator (HSX)].[16]

A stellarator plasma configuration is described by the harmonic spectrum of the magnetic field: $\mathbf{B} = \Sigma \mathbf{B_{mn}} \cos(m\theta - nN_f\phi)$, where N_f is the number of field periods. In magnetic flux coordinates, $\mathbf{B} = \nabla\zeta \times \nabla\psi - q\nabla\theta \times \nabla\psi = \nabla\alpha \times \nabla\psi$, where the field line label $\alpha \equiv \phi - q\theta$ and is a measure of the toroidal location. $2\pi\psi$ represents the poloidal magnetic flux, and $q = q(s)$ is the safety factor, equal to the average number of toroidal circuits traversed by a field line for each poloidal circuit around the torus. An axisymmetric tokamak has all $n \neq 0$ B_{mn} terms negligible; the quasihelical symmetry of HSX requires all B_{mn} terms with $m \neq n$ to be small and the quasiaxially symmetric design of a QAS requires all B_{mn} terms with $n \neq 0$ to be small. The design QAS axial symmetry is broken by $(n \neq 0, m \neq 0)$ components which are ~1% of the strength of the $(n = 0, m = 0)$ component. In Fig. 1 is shown the shape of the last closed flux surface for the QAS, with one half of one field period removed. The cross-section continuously deforms as the toroidal angle changes, as is apparent from the two cross sections shown at the cut. The configuration analyzed, denoted LI383, has a major radius of 1.4 m, an aspect ratio of 4.4, a toroidal magnetic field 1.2–1.7 T and 6 MW of neutral beam heating.

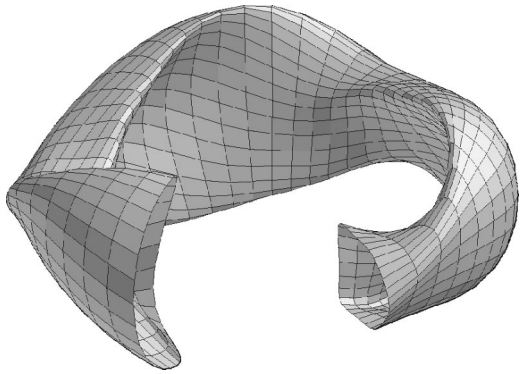

FIG. 1. The outermost flux surface of the three field period quasiaxially symmetric stellarator.

Ballooning mode stability theory is based on the linear, ideal, MHD energy principle, with which minimized plasma energy, δW_p, describes destabilized ballooning and other internal modes

$$\delta W_p = (1/2)\int d\tau [\mathbf{Q}_\perp^2 - j_\parallel(\boldsymbol{\xi}\times\mathbf{B})/B - 2(\boldsymbol{\xi}_\perp\cdot\nabla P)(\boldsymbol{\xi}_\perp\cdot\boldsymbol{\kappa}) + B^2(\nabla\cdot\boldsymbol{\xi}_\perp + 2\boldsymbol{\xi}_\perp\cdot\boldsymbol{\kappa})^2 + \gamma P(\nabla\cdot\boldsymbol{\xi})^2]. \quad (1)$$

In this equation for the variation in plasma energy resulting from a deformation in the plasma flux surface, $\boldsymbol{\xi}$, the first term is the stabilizing magnetic energy of field line bending. The second term is the free energy from the current profile and drives kink instabilities. The third term, proportional to ∇P, is the energy potential for interchange or ballooning instabilities. This term is destabilizing if ∇P and $\boldsymbol{\kappa}$ are in the same direction $(\boldsymbol{\kappa}\cdot\nabla P > 0)$, at the outer edge of a tokamak, for example. The fourth term is the energy in field compression for fast magnetosonic waves and the last term is the energy in compressional sound waves. Minimization of δW_p in the limit as the component of the wave vector perpendicular to $\mathbf{B}$, $k_\perp$, approaches infinity yields a second order ordinary differential Euler–Lagrange equation, if the compressional terms are neglected.

Calculations of ballooning stability provide a relatively simple and rapid method for evaluating the performance of an MHD limited, plasma configuration, and are often used for initial estimates of stability expected for plasma experi-

ments. The ballooning mode is driven by the plasma pressure gradient interacting with the magnetic field. Ions are assumed to have negligible Larmor radius and to be localized to a particular magnetic field line (diamagnetic drift negligible). Although this is a one-dimensional, ideal MHD model, effectively localized to a field line, valid on the Alfvén time scale, with long parallel and short perpendicular wavelength, it contains information about the three-dimensional equilibrium through the plasma equilibrium gradients. The ballooning mode instability eigenvalues, λ, are found by solving the ballooning equation in magnetic coordinates[7]

$$\partial/\partial\theta[(C_p+C_s(\theta-\theta_k)+C_q(\theta-\theta_k)^2)\partial\xi/\partial\theta] + (1-\lambda)[d_p+d_s(\theta-\theta_k)]\xi=0. \quad (2)$$

The coefficients $\{C_p, C_s, C_q, d_p, d_s\}$ depend on the equilibrium magnetic geometry. The coefficients d_s and C_s of the linear secular terms in Eq. (2) are proportional to $q'(s)/\Psi'(s)$, the (global magnetic) shear, while that of the quadratic secular term, C_q, is proportional to the square of the shear. The radial coordinate, s, is the edge normalized toroidal flux, $\Psi(r)/\Psi(a)$, which is proportional to r^2. The parameter θ_k is related to the direction of the mode wave vector. The secular terms cause localization when the shear is nonzero: very roughly, the eigenfunction is localized around $\theta\sim\theta_k$. The calculation results in an eigenvalue at each flux surface which implies instability if positive: $\lambda>0$. The displacement of the flux surface increases with a notional growth rate $\gamma=\sqrt{\lambda}=i\omega$, as $\xi\propto\exp(i\omega t)\propto\exp(\sqrt{\lambda}t)$. The normalization of the kinetic energy on which Eq. (2) is based, leads to isosurfaces valid at the marginal point ($\lambda=0$), and qualitatively correct for unstable values of λ. Further work is needed to verify the structures in the stable spectrum.

The ballooning equation can also be transformed into a Schrödinger-type form[9]

$$[d^2/d\theta^2+E-V]\mathcal{A}^{1/2}\xi=0 \quad (3)$$

with the "potential" V and the coefficient $\mathcal{A}$ expressed in terms of the ballooning coefficients. The secular terms due to magnetic shear provide a "potential well," modulated by the poloidal and toroidal variations in the equilibrium quantities on the given field line. In the axisymmetric case (i.e., no toroidal variation) this shear localization is the only effect giving localization and hence a discrete spectrum in λ: when shear vanishes, V is periodic and the λ spectrum consists of continuum bands ("Brillouin zones"). However, in the non-axisymmetric case the incommensurate periodicity of the toroidal and poloidal modulations (when q is an irrational) can give rise to Anderson localization and a discrete spectrum even when the shear vanishes.

III. BALLOONING MODE SPECTRUM RESULTS AND VISUALIZATION

High-β equilibria for the QAS were obtained with the VMEC code,[17] keeping the fixed boundary coordinates of the marginally stable design point and scaling the pressure and current profiles together. As β increases, the bootstrap current driven by increased plasma pressure causes the poloidal magnetic field and plasma iota to increase. Two such equilibria, confirmed by convergence studies, will be compared, one just above marginal stability at $\beta=4.3\%$ and one far above marginal stability, at $\beta=6.8\%$. These cases are not only ballooning unstable but also Mercier unstable. Figures 2 and 3 show profiles of the pressure derivatives and iota, for these equilibria. The TERPSICHORE code suite module VVBAL[7] was used to find the eigenvalues of the ballooning equation. In Fig. 4 is shown the radial dependence of the growth rates, for a range of betas above the marginal stability point, parametrized by $\alpha=\theta_k=0$.

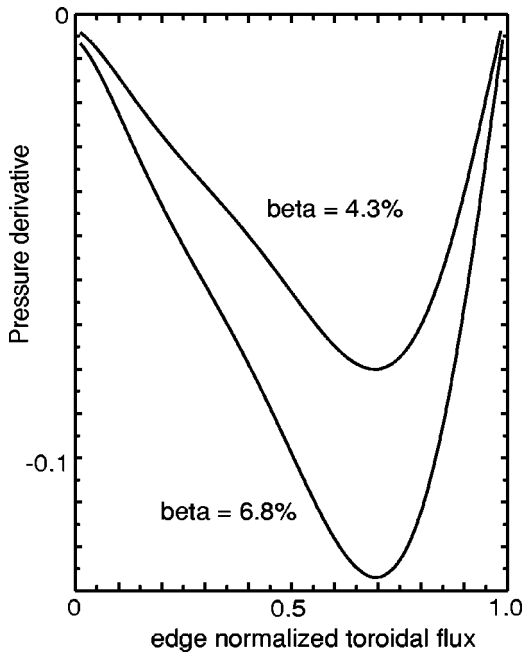

FIG. 2. Derivatives of the pressure profile for two ballooning unstable equilibria of the QAS, obtained with fixed boundary VMEC. Steeper pressure results in higher β, but also drives MHD instability.

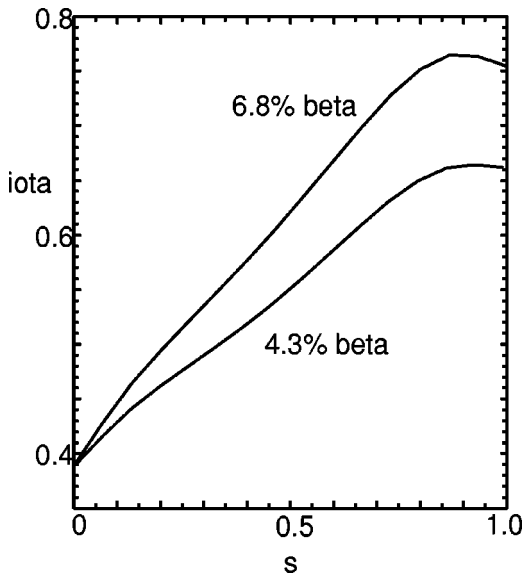

FIG. 3. Iota profiles of two ballooning unstable equilibria of the QAS. Higher pressure drives bootstrap currents which increases the field line transform iota at 6.8% compared to 4.3% β.

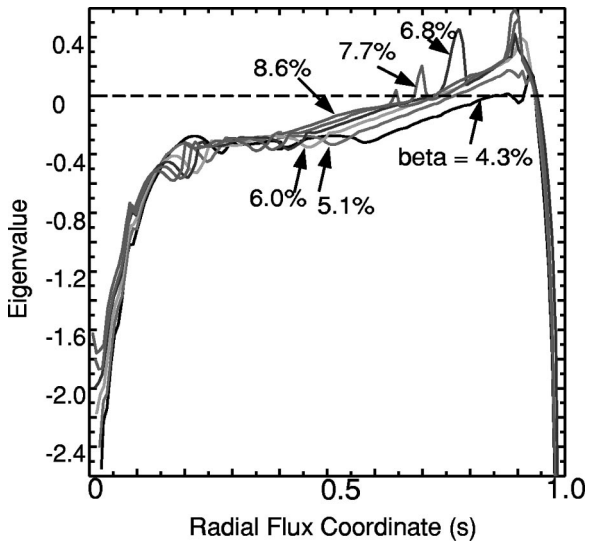

FIG. 4. Ballooning eigenvalues as a function of the radial coordinate for a β scan above the ballooning limit of QAS3_LI383. 129 radial flux surfaces are used. Singular points occur where rational values of q are found and for locations of very low shear.

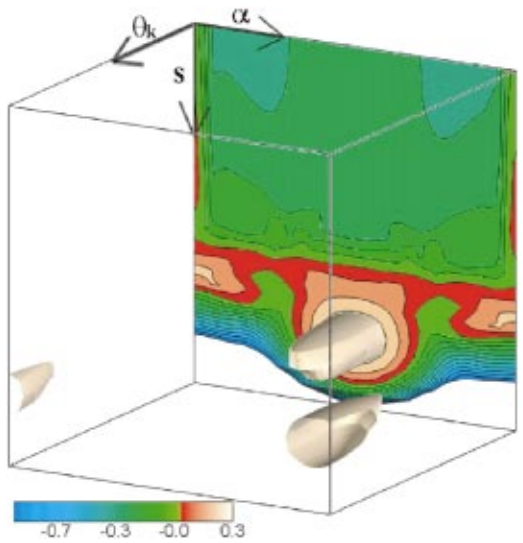

FIG. 5. (Color) Ballooning spectrum of 4.3% β QAS configuration: The eigenvalue isosurface near the plasma edge for the unstable mode at $\lambda(s,\alpha,\theta_k)=0.25$, comprises two topologically spherical surfaces. Also shown is the plane in (s,α) at $\theta_k=0$. The color map at the bottom of the figure identifies stable eigenvalues in blue and green and unstable eigenvalues in red and beige. A cross section of the marginal isosurface is located on the (s,α) plane at the separation between red and green contours. The full 3-space is reduced to show toroidal flux, s, from 0.8 to 1.0; field line variable α from 0 to $2\pi/3$; ballooning parameter θ_k, from 0 to 2π.

The results, $\lambda(s,\alpha,\theta_k)$, of ballooning stability calculations were assembled into databases for the 4.3% and 6.8% β equilibria. Calculations were made for 129 flux surfaces in the radial coordinate, and for 101 values of the parameter α, from 0 to $2\pi/3$, and for 21 values of the parameter θ_k, from 0 to 2π. The resulting three-dimensional isosurfaces $\lambda(s,\alpha,\theta_k)$ for stable ($\lambda<0$) and unstable ($\lambda>0$) ballooning modes show features of localized structures, quite different from those seen for other stellarators or the rippled tokamak.

In Figs. 5 and 6 are shown examples of the three-dimensional structures found at 4.3% β for unstable and stable values of the ballooning eigenvalue. Additional figures illustrating the features described below for the QAS configurations and the tokamak case, with a slightly different colormap, may be viewed at the AIP Electronic Publication Auxiliary Publication Service (EPAPS).[18]

In general the unstable spectra at both 4.3% β and 6.8% β are less complex than the stable spectra. The unstable ballooning spectra consist primarily of bands or continuous tubules of instability near the outer edge of the plasma, where shear is very low and instability is more easily driven. For all cases there is weak dependence on the ballooning angle, stronger dependence on the field line α and strongest dependence on s, the magnetic surface. At 4.3% β, (Fig. 5) we find topologically spherical isosurfaces at $\lambda=0.25$ which become topologically cylindrical surfaces at lower positive λ values. As λ decreases toward 0, the cylindrical surfaces narrow in s and extend toward each other along α, along with the appearance of a connecting plane when $\lambda=0.025$. The marginal isosurface, $\lambda=0$, is shown in Fig. 6 with thickness corresponding to data cube grid spacing, $\Delta s=0.01$: two cylinders connected by a plane. At 6.8% β planar (α,θ_k) isosurfaces are found at $\lambda=0.05$, which break up into shreds as the eigenvalue is increased above 2.4.

In the stable spectra, unusual topologically distinct structures are found in the different ranges of λ, with similar structures occurring for both the low and high-β equilibria. At 4.3% β for $\lambda=-0.2$, the isosurface exhibits a helical structure which rotates about an axis along the θ_k direction. The structure is radially and toroidally localized within a small range of α with the isosurface helix open toward the plasma center. At 4.3% β and $\lambda=-0.45$, stable isosurface tubes are found, again aligned in the θ_k direction, localized in s and α. At 6.8% β, similar isosurface structures in the

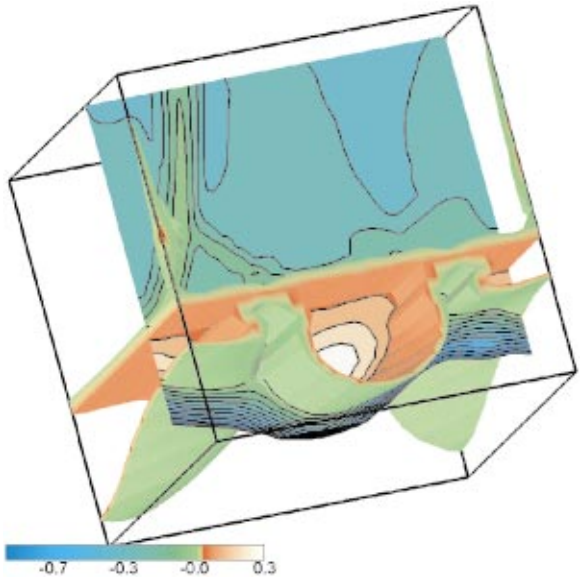

FIG. 6. (Color) Ballooning spectrum of 4.3% β QAS configuration: the marginal isosurface at $\lambda(s,\alpha,\theta_k)=0$, for the same color map and reduced 3-space as in Fig. 5. Also shown is the (s,α) plane at $\theta_k=2\pi/3$.

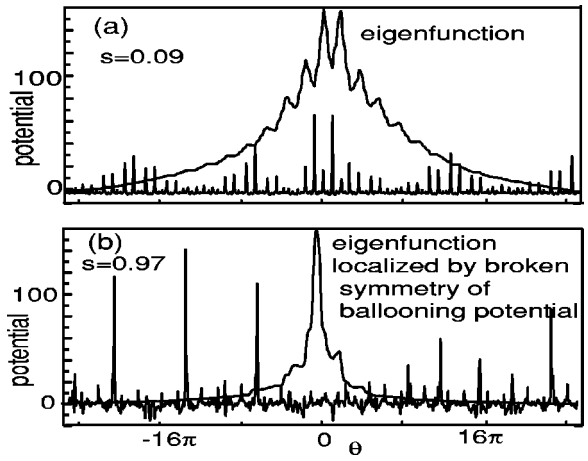

FIG. 7. The localization of the ballooning mode eigenfunction for 4.3% β and the ballooning potentials on flux surfaces near the magnetic axis and the plasma edge. The eigenfunctions are normalized to the same maximum value. The ballooning potential is increasingly aperiodic far from the magnetic axis, where axial symmetry is more strongly broken.

stable spectrum occur, although more global in extent, and located at two planes in *s*, corresponding to low order rational flux surfaces (see Figs. 3 and 4). The complex structure of the datacube for the QAS ballooning mode spectra has been examined with the powerful visualization tool, AVS-EXPRESS.

When the maximum eigenvalue for all flux surfaces is plotted for the 4.3% β case, the usual choices ($\theta_k=0, \alpha=0$) are found to correspond to average levels of instability and do not represent anomalously low or high eigenvalues. Stellarator symmetry is apparent with reflection about $\alpha=\pi/6$ and $3\pi/6$. The alpha dependence of the eigenvalue for the 4.3% β equilibrium repeats after $2\pi/3$ and is symmetric about $\alpha=0$, $\pi/3$, $2\pi/3$, $3\pi/3$, etc. Contours of unstable eigenvalues for both equlibria show the localization in α and *s* of the unstable modes.

In Fig. 7 is shown the ballooning eigenfunction and potential, *V*, of Eq. (3), for flux surfaces near the magnetic axis and the plasma edge. Eigenfunction localization is seen to increase near the plasma edge where the magnetic shear is weak or zero. Similar low-shear localization of the eigenfunction was also found by Dewar and Cuthbert[9] for the H-1NF heliac. They showed that the localization was not due to magnetic shear by setting it artificially to zero, instead attributing it to Anderson localization.

For the stable and unstable spectra of equilibria above the ballooning limit, there is weak dependence of $\lambda(s,\alpha,\theta_k)$ on the ballooning angle, strong dependence on the field line alpha and strongest dependence on *s*, the magnetic surface radial coordinate. These findings are similar to those from the ballooning stability analysis[9] for H-1NF, while the 10 field period stellarator ballooning stability datacube[10] showed stronger dependence on θ_k and *s*, but weak dependence on α. While localized structures have been found for the 10 field period stellarator, for Heliotron-J[19] and the H-1NF heliac, it is somewhat surprising to find them also in the QAS because this is supposed to have tokamak-like properties.

The QAS is next compared to a related axisymmetric case. A plasma equilibrium based on the pressure and boundary parametrizations used for the 4.3% β QAS configuration, is obtained, keeping only toroidal $n=0$ plasma major radius and boundary harmonics. This leads to a two-dimensional equilibrium, $\beta=7\%$, with similar values of *B*, *A*, R_{axis}. The field line transform, iota, is much lower [$\iota(0)=0.02$, $\iota(1)=0.22$] because there is no external transform as previously provided by the stellarator coils and described by three-dimensional boundary coefficients. A distinct difference in the isosurfaces $\lambda(s,\alpha,\theta_k)$ and the ballooning mode stability is found as expected. Most dramatic is the simplicity of the tokamak isosurface structures. The axisymmetric case shows no α dependence, no toroidal localization, as there are no driving terms with this symmetry.

IV. DISCUSSION AND CONCLUSION

In solutions of the ballooning equation, expected to limit high β performance for the compact quasiaxially symmetric stellarator, we find toroidal localization of ballooning mode eigenvalue isosurfaces with new, topologically distinct structures not seen in previous studies of other stellarator configurations. The relative complexity of the QAS ballooning spectrum isosurfaces for NCSX is driven by the complexity of the magnetic configuration, since boundary coefficients with only $n=0$ components lead to isosurfaces with no toroidal dependence. Anderson localization and spherical isosurfaces, indicative of strong quantum chaos, have been identified and are discussed below.

Anderson localization occurs in response to broken symmetry (here axisymmetry), as seen in the localization of electron wave functions in disordered solids. It was first identified as localized structures in the electron conduction band arising from disorder in a crystalline matrix due to impurity doping. In one-dimensional quantum systems it is now well known that disorder results in normal modes that are exponentially localized. In plasmas several authors[20,21] have shown that Anderson localization arises from quasiperiodicity of equilibrium quantities along a field line.

The iota profiles in Fig. 3 show weak and reversed shear near the QAS plasma edge. Weak shear reduces the strength of the secular terms, $\sim(\theta-\theta_k)$, in the ballooning equation (2), which in axisymmetric systems are responsible for localization of the ballooning eigenfunction. In contrast, localization of the QAS ballooning eigenfunction increases in regions of reduced plasma shear as seen in Fig. 7, demonstrating that something other than the well known shear localization is responsible. In fact the eigenfunction becomes most peaked where plasma shear is zero, at the surface where $\iota=0.631$. The eigenfunctions for the 4.3% case are shown for $\theta_k=0$. Each surface has a different shape so that the poloidal angle at which the eigenfunction is maximum changes with *s*. Localization correlates with increasing aperiodicity of the ballooning potential (Fig. 7). The effective toroidal ripple,[22] which is one measure of this breaking of axisymmetry, changes by nearly three orders of magnitude across the plasma (Fig. 8). We conclude that as has been

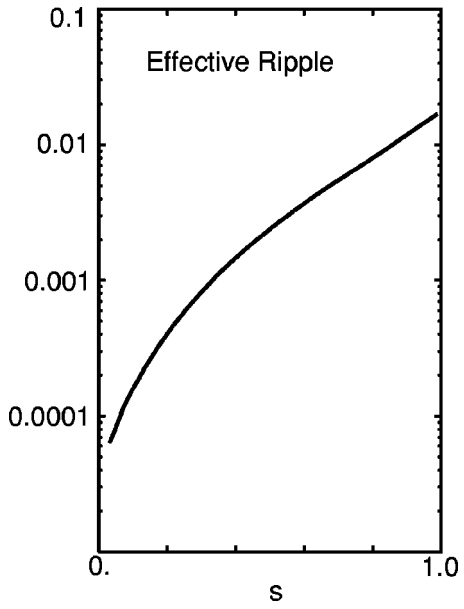

FIG. 8. Effective field line ripple for the QAS at 4.3% β.

found in H-1NF and HSX, the QAS also exhibits Anderson localization, occurring where shear is reduced and axial symmetry is broken.

At 4.3% β, at the highest eigenvalues, we have found topologically spherical isosurfaces. Ray tracing in such cases shows strong ''quantum chaos.''[23] This description for the paths of rays of high-$k_\perp$ MHD waves or instabilities does not mean that the plasma behavior is chaotic, but that the mathematics of quantum chaos theory must be used for instabilities far above the marginal point of the equilibrium. An additional complication in using ideal MHD with ray tracing to construct global ballooning modes is a *k*-space runaway. Introduction of a reflecting cutoff in $k_\perp$ to model numerical truncation or finite Larmor radius (FLR) yields chaotic ray paths ergodically filling the allowed phase space, indicating that the global spectrum must be described using the language of quantum chaos theory.

Can the Dewar–Glasser[8] WKB ballooning mode method still be used to estimate the β limit of the QAS? A necessary condition for the validity of ideal MHD ballooning theory is that the equilibrium scale length, L_{eq}, be much larger and the ion gyroradius, ρ_i, much smaller than $k_\perp$, the perpendicular wavelength: $k_\perp L_{\mathrm{eq}} \gg 1, (k_\perp \rho_i)^2 \ll 1$. For the NCSX QAS, $\rho_i \sim 1$ cm. For some stellarator equilibria, $k_\perp$ has been estimated from the isosurface structures, making use of the method of WKB ray tracing[9,10] and derivation of semiclassical quantization conditions for the eigenfunction. In contrast, for the spherical isosurfaces of high eigenvalue surfaces of H-1NF, the mathematics of quantum chaos and statistical density of states was needed. To examine the validity of the ballooning mode β limit, it is the marginal isosurface, $\lambda = 0$, which is of interest. At both 4.3% β and at 6.8% β we find that this surface is not simply connected. At 4.3% β, it consists of a planar surface tangent to two topologically cylindrical surfaces, with axes parallel to θ_k. Other stellarators have also been found to have topologically cylindrical surfaces, but with axis aligned in the α-direction, not along θ_k. Work is in progress to develop new methods for regularizing the WKB ray tracing and quantization conditions in this case, to estimate $k_\perp$ and possible FLR stabilization. The ray tracing for the QAS surfaces may not follow simple paths, as the rays may trace out paths on either or both of the cylinders, transiting through the connecting plane and moving onto and off the cylinders in a random and stochastic fashion. The complexity of the marginal isosurface suggests that the WKB method of high-*n* ballooning stability calculations breaks down, and that fully three-dimensional, MHD codes such as CAS3D, TERPSICHORE and Spector3D are required to predict a maximum β for the QAS.

Can this new way of looking at a stellarator provide insight into improving the QAS concept? The QAS, with a complex harmonic magnetic spectrum, exhibits complex localized, unstable isosurface structures for the MHD ballooning modes, which will also affect calculations of the anomalous transport of particles and kinetic energy in the QAS, for example, with gyrokinetic ballooning calculations.[24] For representative nonaxisymmetric cases, collisionless, electrostatic drift mode calculations have shown large (factors >2) changes in instability growth rates, which depend on the field line variable α.[25,26] To achieve optimal stellarator performance it will be important to verify that the complex magnetic spectrum, which provides good neoclassical particle confinement and MHD stability, does not cause unacceptable increases in anomalous transport.

ACKNOWLEDGMENTS

We would like to thank M. C. Zarnstorff, C. Hegna, and L.-P. Ku for discussions and S. P. Hirshman for use of the VMEC code.

Research supported by U.S. DOE Contract No. DE-AC02-76CH0373. John Canik held a U.S. DOE National Undergraduate Fellowship at Princeton Plasma Physics Laboratory, during the summer of 2000.

[1] J. Nührenberg, W. Lotz, and S. Gori, in *Theory of Fusion Plasmas*, edited by E. Sindoni, F. Troyon, and J. Vaclavik (Societa Italiana di Fisica, Bologna, 1994), p. 3.
[2] P. R. Garabedian, Phys. Plasmas **3**, 2483 (1996).
[3] E. Noether, *Invariante Variationsprobleme*, Nachr. D. Koenig. Gesellsch. D. Wiss. Zu Goettingen, Math-phys. Klasse (1918), pp. 235–237.
[4] M. C. Zarnstorff, L. A. Berry, A. Brooks *et al.*, ''Physics of compact advanced stellarators,'' Plasma Phys. Controlled Fusion (in press).
[5] W. A. Cooper, D. B. Singleton, and R. L. Dewar, Phys. Plasmas **3**, 275 (1996).
[6] C. Nührenberg, Phys. Plasmas **3**, 2401 (1996); C. Schwab, Phys. Fluids B **5**, 3195 (1993).
[7] W. A. Cooper, Plasma Phys. Controlled Fusion **34**, 1011 (1992).
[8] R. L. Dewar and A. H. Glasser, Phys. Fluids **26**, 3038 (1983).
[9] P. Cuthbert and R. L. Dewar, Phys. Plasmas **7**, 2302 (2000).
[10] P. Cuthbert, J. L. V. Lewandowski, H. J. Gardner, M. Persson, D. B. Singleton, R. L. Dewar, N. Nakajima, and W. A. Cooper, Phys. Plasmas **5**, 2921 (1998).
[11] S. M. Hamberger, B. D. Blackwell, L. E. Sharp, and D. B. Shenton, Fusion Technol. **17**, 123 (1990).
[12] J. Chen, N. Nakajima, and M. Okamoto, Phys. Plasmas **6**, 1562 (1999).
[13] A. Iiyoshi and K. Yamazaki, Phys. Plasmas **2**, 2349 (1995).
[14] P. W. Anderson, Phys. Rev. **109**, 1492 (1958).
[15] C. Beidler, G. Greiger, F. Herrnegger *et al.*, Fusion Technol. **17**, 148 (1990).
[16] D. T. Anderson, A. F. Almagri, F. S. B. Anderson, P. H. Probert, J. L. Shohet, and J. N. Talmadge, J. Plasma Fusion Res. **1**, 49 (1998).

[17]S. P. Hirshman and O. Betancourt, J. Comput. Phys. **96**, 99 (1991).
[18]See EPAPS Document No. E-PHPAEN-9-911205 for additional figures of $\lambda(s,\alpha,\theta_k)$. This document may be retrieved via the EPAPS homepage (http://www.aip.org/pubservs/epaps.html) or from ftp.aip.org in the directory /epaps/. See the EPAPS homepage for more information.
[19]O. Yamagishi, Y. Nakamura, and K. Kondo, Phys. Plasmas **8**, 2750 (2001).
[20]R. L. Dewar and P. Cuthbert, Chin. Phys. Lett. **0256-307X**, 33 (2000).
[21]C. Hegna and S. Hudson, Phys. Rev. Lett. **87**, 035001 (2001).
[22]V. V. Nemov, S. V. Kasilov, W. Kernbichler, and M. F. Heyn, Phys. Plasmas **6**, 4622 (1999).
[23]R. L. Dewar, P. Cuthbert, and R. Ball, Phys. Rev. Lett. **86**, 2321 (2000).
[24]M. Kotschenreuther, W. Dorland, M. A. Beer, and B. W. Hammett, Phys. Plasmas **2**, 2381 (1995).
[25]G. Rewoldt, L.-P. Ku, W. M. Tang, and W. A. Cooper, Phys. Plasmas **6**, 4705 (1999).
[26]G. Rewoldt, L.-P. Ku, W. M. Tang *et al.*, Phys. Plasmas **7**, 4942 (2000).